Negative-curvature Anti-resonant Fiber Coupling Tolerances

This article has been accepted for publication in a future issue of this journal, but has not been fully edited. Content may change prior to final publication. Citation information: DOI 10.1109/JLT.2019.2937210, Journal of Lightwave Technology

Negative-curvature Anti-resonant Fiber Coupling Tolerances

Bartłomiej Siwicki, Richard M. Carter, Jonathan D. Shephard, Fei Yu, Jonathan C. Knight, and Duncan P. Hand

***Abstract*—We investigate coupling tolerances of selected designs of negative-curvature anti-resonant fibers (NC-ARFs) with open- and closed-boundary types of structure under linear and angular misalignment of the input near-infrared laser beam. The coupling tolerances of NC-ARFs are compared with those of a commercially available step-index fiber. The expected coupling efficiency for the step-index fiber is calculated using scalar diffraction theory and directly compared with measured profiles. We show that the analyzed NC-ARFs can provide lower sensitivity to input beam misalignment than the step-index fiber, despite having a numerical aperture approximately half of that of the step-index fiber (0.044 compared to 0.07 respectively). In particular, a nodeless design is only half as sensitive to input linear misalignment than the step-index fiber, whilst having an almost identical sensitivity to tilt. A 3.5 µm linear shift and 22 mrad tilt result in 10% decrease in total output power of the beam. The good match between experiment and calculations suggests that the profiles measured for NC-ARFs are correct.**

***Index Terms*—negative-curvature anti-resonant fiber, high-power beam delivery, coupling efficiency.**

I. Introduction

VARIOUS designs of hollow-core optical fibers have been in use for many years. In principle, they allow propagation with both ultra-low loss and ultra-low nonlinearity by guiding light in air rather than in a solid material. They also provide significantly higher laser-induced damage thresholds than solid-core fibers and can transmit at wavelengths at which the cladding material is strongly absorbing. In particular, the relatively new negative-curvature anti-resonant fibers (NC-ARFs) can have exceptionally high laser damage thresholds, thanks to a very small area of overlap between the propagating core mode and surrounding glass cladding structure [1], [2]. They can also transmit UV, as well as near- and mid-IR wavelengths with an attenuation as low as 1.3 dB/km at λ = 1550 nm or 34 dB/km at λ = 3.05 µm [3], [4], [5], [6], [7]. NC-ARFs are hence very promising for high-power laser beam delivery, and indeed ultra-short pulsed flexible delivery systems based on these fibers have been commercialised [8].

However, in order to obtain a high damage threshold the laser-fiber coupling arrangement and coupling efficiency are vitally important. Angular or linear misalignment of the input beam causes excitation of higher-order modes or distortion of the fundamental mode, as has been shown e.g. in [2] or [9]. In both cases, part of the energy of the excited mode is shifted to the proximity of glass walls as opposed to the undistorted LP_{01} mode, thus decreasing the fiber's damage threshold and overall output transmission.

Numerous fiber designs with nested capillaries or multiple cores have been also studied to tackle the problem of confinement losses and bend sensitivity of NC-ARFs [4], [9], [10] or [11]. Although nested-capillaries fiber designs can provide lower transmission loss, low bend loss and effective single-mode operation, they cannot be reliably fabricated and are not yet commercially available.

We present a detailed study of the coupling efficiency of selected NC-ARFs as a function of lateral, longitudinal and angular misalignment of the input beam at 1064 nm wavelength. NC-ARFs with two different lattice structures have been investigated – an NCF "ice-cream cone"-type fiber and a nodeless open-boundary (OBF-type) fiber, together with a standard single mode step-index fiber as a benchmark. To the best of our knowledge, the impact of input coupling misalignment on the coupling efficiency of NC-ARFs has not been yet thoroughly investigated. We concentrated on well-established fiber designs, which can be reliably fabricated and are already commercially available.

II. Investigated Fibers

Two types of NC-ARFs have been selected for investigation. The first fiber is an "ice-cream cone"-type of fiber referred to below as "NCF" (Fig. 1(a)). It has a 25.0 µm core, measured as a diameter of the inscribed circle, NA = 0.044 and capillaries with a wall thickness of 850 nm. The second fiber is referred to as "OBF" (Fig. 1(b)). It has a 23.8 µm core diameter, NA = 0.044 and capillaries of wall thickness 210 nm. As a

This work was supported by projects EP/M025888/1, EP/I01246X/1, EP/M025381/1, and EP/I011315 financed by Engineering and Physical Sciences Research Council, UK.

B. Siwicki, R. M. Carter, J. D. Shephard, and D. P. Hand are with Heriot-Watt University, Institute of Photonics and Quantum Sciences, Edinburgh Campus, EH14 4AS Edinburgh, UK (e-mail: b.siwicki@hw.ac.uk; r.m.carter@hw.ac.uk; j.d.shephard@hw.ac.uk; d.p.hand@hw.ac.uk).

F. Yu was with the Centre for Photonics and Photonic Materials, Department of Physics, University of Bath, BA2 7AY Bath, UK. He is now with the Shanghai Institute of Optics and Fine Mechanics, Chinese Academy of Sciences, 390 Qinghe Rd, Jiading Qu, Shanghai Shi, China (e-mail: yufei@siom.ac.cn).

J. C. Knight is with the Centre for Photonics and Photonic Materials, Department of Physics, University of Bath, BA2 7AY Bath, UK (e-mail: j.c.knight@bath.ac.uk).

benchmark, a 1060XP step-index fiber from Thorlabs with a 5.8 μm core diameter and NA = 0.14 has been used [12], referred to as "step-index". The values of NA are given for half-angle of divergence of the beam.

The attenuation of both NC-ARFs at 1064 nm measured with the cutback method is 25 dB/km and 0.5 dB/m respectively (Fig. 2). The fiber lengths used for this measurement were 45 m of the NCF and 43.8 m of the OBF respectively. It is worth mentioning that the OBF fiber was originally designed to operate at 532 nm, but has been selected for this experiment due to its achievable overall transmission of more than 90%. The step-index fiber is specified to have <2 dB/km attenuation at λ = 1064 nm.

III. Measurement setup and conditions

A schematic of the measurement setup is shown in Fig. 3. The measurement light source is a CW laser diode LCM-T-112 supplied by Laser-export Co. Ltd, operating at a wavelength of 1064 nm. The beam quality was assured by using a spatial filter with a 250 μm diameter pinhole. The laser beam was then collimated, providing a beam of 1.4 mm diameter. By selecting an appropriate focusing lens L3 together with a suitable telescope magnification the effective NA of the input beam was matched with the NA of the particular fiber being investigated. The required combination differs for the step-index fiber and the ARFs due to the significant difference in NA (0.07 for the step-index and ~0.044 for the ARFs. In order to precisely align the fibers a 6-axis motorized NanoMAX stage (Thorlabs) was used, which can be positioned with linear and angular accuracies of 250 nm and 180 μrad, respectively. The output power was measured using a Si photodiode. The total loss introduced by the various optical components was 13.2%.

The experimental procedure was as follows. As a reference, the optical power just before the fiber was measured. The fiber was then mounted on the 6-axis stage, and the maximum transmission was obtained by precisely adjusting the linear position and angular alignment of the fiber. In order to optimise the 1064 nm laser-fiber coupling, light from a 532 nm laser diode was coupled into the other end of the fiber. Then, the two counter-propagating beams (IR and green) at the input end were made co-linear by careful adjustment of the input mirrors *M* to ensure proper inclination of the input beam in regards to the fiber face. Finally, the fiber position was re-adjusted to achieve the best transmission. In both NC-ARFs a single mode with a Gaussian-like energy distribution was excited in the core area at 1064 nm wavelength (Fig. 4). The mode was localized slightly off-centre by a few microns, likely due to small cladding imperfections, such as variation in size and separation of the capillaries surrounding the core [2] or due to small bend of the fiber [13]. The step-index fiber has a cut-off wavelength of 920 nm, thus was purely single-mode at 1064 nm wavelength.

The main experiment was divided into two parts. In the first part, in order to record the loss in output transmission due to input linear coupling misalignment, all three analysed fibers were shifted by steps of 250 nm in the horizontal *X* and vertical *Y* axes, and by steps of 15 μm in the longitudinal *Z* axis. In the second part, the stage was tilted by increments of 900 μrad in both the negative and positive directions around the *X* axis in the *YZ* plane (see Fig. 3). The resulting misalignment of the fiber tip in case of tilting would be purely angular only if the tip was placed precisely at the fixed-point of rotation of the 6-axis stage, which, although great care was taken, was not possible to achieve in this case. Hence a linear shift of the tip also occurred, and so the vertical *Y* axis was re-adjusted after each step. In all cases, the position of the stage at which the total transmission was maximum is defined as zero. Finally, the expected transmission loss in the step-index fiber was calculated based on scalar diffraction theory and compared with the experiment.

IV. Experimental results

All three fibers were measured using the same procedure, starting from a misaligned position of minimal output power and moving towards the optimum position and maximum signal. The *Z* axis position was initially adjusted using a 15 μm step, then as the signal increased rapidly, this step size was reduced to 3 μm (for the last 75 μm of movement). The tested length of fibers was: 1 m of NCF, 40 cm of OBF, <10 m of the step-index respectively.

The measured transmission loss in the NCF, normalized to the maximum value is plotted as a function of lateral and longitudinal input misalignment in Fig. 5. The maximum output transmission obtained in the fiber was 86%. Based on the measured attenuation (Fig. 2), at 1064 nm the expected loss introduced by the 1 m NCF sample in this case was 0.5%, hence the lowest coupling loss is 13.5%.

For lateral misalignments there is a visible difference in transmission loss for the two axes, with the *X* axis being more sensitive for coupling misalignment than the *Y* axis (Fig. 5(a)). Shifts of 1.76 μm (*X*) and 2.50 μm (*Y*) cause a 10% power loss. The difference possibly stems from imperfections of the capillaries on one side of the fiber structure or input beam tilt with respect to the optical axis of the lens. In case of the longitudinal direction *Z*, a 48 μm shift causes a 10% loss of power (Fig. 5(b)). For the angular misalignment, meanwhile, a 10.5 mrad tilt causes a 10% power loss (Fig. 5(c)).

The measured transmission loss normalized to maximum as a function of input misalignment for the OBF fiber is presented in Fig. 6. The maximum obtained transmission was 90%, and given that it is expected that a 5% loss would be introduced by the 40 cm length of OBF at this wavelength that the lowest coupling loss was only 5%.

As can be seen in Fig. 6(a), the transmission loss characteristics for both the *X* and *Y* axes in the OBF fiber are well-matched. Lateral shifts of 3.40 μm (*X*) and 3.50 μm (*Y*) cause a 10% power loss, whilst in a 63 μm shift is required for

the same loss in the longitudinal direction Z (Fig. 6b). For angular misalignment, a tilt of 22 mrad (Fig. 6(c)) is required for 10% loss. All of these values are larger for the OBF than the NCF, demonstrating that it is less sensitive to misalignment.

For reference to the above results, the measurement of transmission loss as a function of input misalignment has been repeated for a "well-known" type of fiber - the step-index fiber. The analysed sample length was <10 m and the maximum obtained transmission was 69%. The total output transmission for the step-index fiber was lower than expected most likely due to slight angular deviation of the input beam introduced by the change of magnification of the telescope, for which it was difficult to precisely compensate. The comparison of transmission losses obtained for all three investigated fibers is presented in Fig. 7.

The results presented in Fig.7 demonstrate that the NC-ARFs are less sensitive to linear misalignments but more sensitive to tilting than the step-index fiber. Interestingly, however, the OBF fiber, although only half as sensitive to linear input misalignment than the step-index fiber, was only slightly more sensitive to tilt (by 2.5 mrad). The difference in sensitivity of coupling misalignment between NC-ARFs and conventional step-index fiber stems from the difference between their structures and physics of operation. The main factors here are the core-cladding refractive index difference, core size and the refractive index distribution of the core. Additionally, step-index fibers provide guidance via total internal reflection of light from the interface between the core and the cladding area, while anti-resonant fibers do not require a specific angle of incidence of light on the air-glass interface in order for them to work. Therefore, the analysed NC-ARFs with their larger core sizes and guidance based on the anti-resonance effect are less sensitive to linear misalignment than the step-index fibers. At the same time, given their lower NA values, they are more sensitive to tilting than the step-index fiber.

The biggest difference in coupling efficiency among the analysed fibers could be seen in case of tilt (Fig. 7(d)). The OBF fiber, that has a cladding made of separate capillaries, had a much lower sensitivity to misalignment than the NCF fiber, despite having a similar NA. This possibly stems from the lack of glass nodes (which can act as waveguides) and wide separation of the capillaries in the OBF (see Fig. 1(b)), coupled with the slightly smaller core area than the NCF fiber.

To confirm this theory, three other NCF- and OBF-types of fiber with similar core sizes but various spacing between capillaries were tested for the tilt sensitivity. The results are presented in Fig. 8. The presented results confirm that the OBF fiber with well-separate capillaries is much less sensitive to tilt (red curve in Fig. 8) than fiber structures having glass nodes or less spaced capillaries. The explanation of this phenomenon is that the OBF fiber design was not optimized for highly single-mode performance, so higher-order modes exhibit weaker suppression. Therefore, offset launch conditions instead of reducing intensity of the fundamental mode excite higher-order modes (also observed in [2]), which then prolong light propagation and decrease the rate at which the output power decreases.

A practical measure of sensitivity to alignment is the fiber tip position shift that results in a 10% decrease in the output beam power for three investigated fibers. This is presented in Table 1 and Fig. 9. The investigated NC-ARFs have in general at least 50% lower sensitivity to input linear coupling misalignment than the step-index fiber, but with the OBF fiber a similar sensitivity to angular misalignment.

V. Theoretical Calculations

Scalar diffraction theory may be used to calculate the expected coupling efficiency in the step-index fiber [14]. A linear misalignment of the input end of the fiber from the paraxial image position given by the focusing lens can be represented as aberrations of the beam in the exit pupil plane of the fiber. If the misalignments are shifts δx and δy in the X and Y axis respectively, and δR in the Z axis, then the corresponding contributions to the aberrations are:

$$W_{1x} = \frac{\delta x h_s'}{R'}, W_{1y} = \frac{\delta y h_s'}{R'}, W_{20} = \frac{\delta R h_s'^2}{2R'^2}, \quad (1)$$

where h_s' is the half-width of the source (radius of the collimated beam), and R' is the distance from the focusing lens.

With the assumption that the input beam lies on the optical axis of the focusing lens, so that only spherical aberration and fiber misalignments contribute to coupling losses, the general coupling efficiency for linear misalignments of the fiber can be expressed as

$$T = A \cdot \exp\left\{-B\left[\left(\pi\frac{W_{1x}}{\lambda}\right)^2 + \left(\pi\frac{W_{1y}}{\lambda}\right)^2\right]\right\}, \quad (2)$$

where

$$A = \frac{\sigma^2}{\beta^2 + (\pi W_{20}/\lambda)^2}, B = \frac{\beta}{\beta^2 + (\pi W_{20}/\lambda)^2} \quad (3)$$

and $\beta = (1+\sigma^2)/2$, while $\sigma = h_s'/h_r'$, where h_r' is the half-width of the fiber far-field distribution. The parameter σ represents size mismatch of the two Gaussian distributions. For our calculations σ can be assumed to be equal 1, the beam radius h_s' was 0.45 mm, while focal length of the lens was R' = 6.24 mm.

Meanwhile, angular misalignments of the fiber can be represented by a lateral shift of the fiber exit-pupil distribution. If the angular misalignments are $\delta\theta_x$ and $\delta\theta_y$, then the corresponding normalized exit-pupil shifts are

$$x_0 = \frac{R' sin\delta\theta_x}{h_s'}, y_0 = \frac{R' sin\delta\theta_y}{h_s'}. \quad (4)$$

The resulting coupling efficiency is

$$T = A \cdot \exp[-C(x_0^2 + y_0^2)], \quad (5)$$

where $A = \sigma^2/\beta^2$, and $C = \sigma^2/\beta$.
The calculated coupling efficiency as a function of input linear and angular misalignment of the fiber, along with the measured profile for the step-index fiber are presented in Fig. 10 and Fig. 11 respectively.

A very good match between experiment and theory has been obtained for the *Y* axis (Fig. 10(b)) and the tilt (Fig. 11). The expected coupling loss for the *X* axis (Fig. 10(a)) should have been the same as for the *Y* axis. The observable difference in case of the *X* axis could stem from the possible small tilt of the input beam in the yaw direction introduced by the telescope, causing additional aberrations to the setup and a change in rate at which the transmission decreases. The discrepancy between the experiment and calculations for the *Z* axis most likely resulted from inaccuracy of the input beam size adjustment, provided by the telescope (Fig. 10(c)). Since the size of the beam h_s' in case of focal shift is to the second power in (1), then any error in determining the h_s' has strong impact on the numerical result of coupling efficiency *T* in (2).

The good match between calculations and experiment for the *Y* axis and the tilt in case of the step-index fiber suggests that the profiles measured for NCF and OBF fibers are correct. The perpendicular axis discrepancies probably stemmed from the inaccuracy of input beam alignment in relation to the optical axis of the focusing lens.

VI. Conclusions

The results clearly demonstrate that it is possible to obtain very low loss coupling into NC-ARF's, whilst having a sensitivity to misalignment, either angular or tilt, that is not appreciably worse than standard single mode fiber, although with some subtle differences. Hence standard alignment technologies developed for telecommunications can be used with these novel fibers, albeit with modifications in order to cope with higher laser power levels.

The nodeless OBF performs particularly well; it is only half as sensitive to linear input beam misalignment as the step-index fiber, whilst having an almost identical sensitivity to tilt. Key factors that likely contribute to its better performance are smaller core size, smaller nodeless capillaries and thinner capillary walls than the NCF fiber, which result in a lower effective refractive index of the mode and its better confinement in the core area.

References

[1] J. D. Shephard, A. Urich, R. Carter, P. Jaworski, R. R. J. Maier, W. Belardi, F. Yu, W. J. Wadsworth, J. C. Knight, and D. P. Hand, "Silica hollow core microstructured fibers for beam delivery in industrial and medical applications," *Front. Phys.*, vol. 3, no. 24, 2015.

[2] M. Michieletto, J. K. Lyngsø, C. Jakobsen, J. Lægsgaard, O. Bang, and T. T. Alkeskjold, "Hollow-core fibers for high power pulse delivery," *Opt. Express*, vol. 24, no. 7, pp. 7103-19, 2016.

[3] F. Yu, M. Cann, A. Brunton, W. J. Wadsworth, and J. C. Knight, "Single-mode solarization-free hollow-core fiber for ultraviolet pulse delivery," *Opt. Express*, vol. 26, no. 8, pp. 10879-87, 2018.

[4] T. D. Bradley, J. R. Hayes, Y. Chen, G. T. Jasion, S. R. Sandoghchi, R. Slavik, E. N. Fokoua, S. Bawn, H. Sakr, I. A. Davidson, A. Taranta, J. P. Thomas, M. N. Petrovich, D. J. Richardson, and F. Poletti, "Record Low-Loss 1.3dB/km Data Transmitting Antiresonant Hollow Core Fibre," in 2018 European Conference on Optical Communication (ECOC), pp. 1–3, 2018.

[5] F. Yu, W. J. Wadsworth, and J. C. Knight, "Low loss silica hollow core fibers for 3–4 μm spectral region," *Opt. Express*, vol. 20, no. 10, pp. 11153-8, 2012.

[6] A. N. Kolyadin, A. F. Kosolapov, A. D. Pryamikov, A. S. Biriukov, V. G. Plotnichenko, and E. M. Dianov, ""Light transmission in negative curvature hollow core fiber in extremely high material loss region," *Opt. Express*, vol. 21, no. 8, pp. 9514–9, 2013.

[7] A. F. Kosolapov, A. D. Pryamikov, A. S. Biriukov, V. S. Shiryaev, M. S. Astapovich, G. E. Snopatin, V. G. Plotnichenko, M. F. Churbanov, and E. M. Dianov, "Demonstration of CO2-laser power delivery through chalcogenide-glass fiber with negative-curvature hollow core," *Opt. Express*, vol. 19, no. 25, pp. 25723–8, 2011.

[8] Photonic Tools, *Laser light cable for industrial ultrafast lasers LLK-UKP*. [Online]. Available: https://www.photonic-tools.de/products/llk-ultrafast/.

[9] S. Gao, Y. Wang, W. Ding, D. Jiang, S. Gu, X. Zhang, and P. Wang, "Hollow-core conjoined-tube negative-curvature fibre with ultralow loss," *Nat. Commun.*, vol. 9, 2828, 2018.

[10] M. S. Habib, J. E. Antonio-Lopez, C. Markos, A. Schülzgen, and R. Amezcua-Correa, "Single-mode, low loss hollow-core anti-resonant fiber designs," *Opt. Express*, vol. 27, no. 4, pp. 3824–36, 2019.

[11] X. Huang, J. Zang, and S. Yoo, "Multiple hollow-core anti-resonant fiber as a supermodal fiber interferometer", *Sci. Rep.*, vol. 9, 9342, 2019.

[12] Thorlabs, *1060XP - Single Mode Optical Fiber*. [Online]. Available: https://www.thorlabs.com/thorproduct.cfm?partnumber=1060XP.

[13] P. Jaworski, F. Yu, M. Carter, J. C. Knight, J. D. Shephard, and D. P. Hand, "High energy green nanosecond and picoseconds pulse delivery through a negative curvature fiber for precision micro-machining," *Opt. Express*, vol. 23, no. 7, pp. 8498-506, 2015.

[14] R. E. Wagner, and W. J. Tomlinson, "Coupling efficiency of optics in single-mode fiber components," *Appl. Optics*, vol. 21, no. 15, pp. 2671-88, 1982.

This article has been accepted for publication in a future issue of this journal, but has not been fully edited. Content may change prior to final publication. Citation information: DOI 10.1109/JLT.2019.2937210, Journal of Lightwave Technology

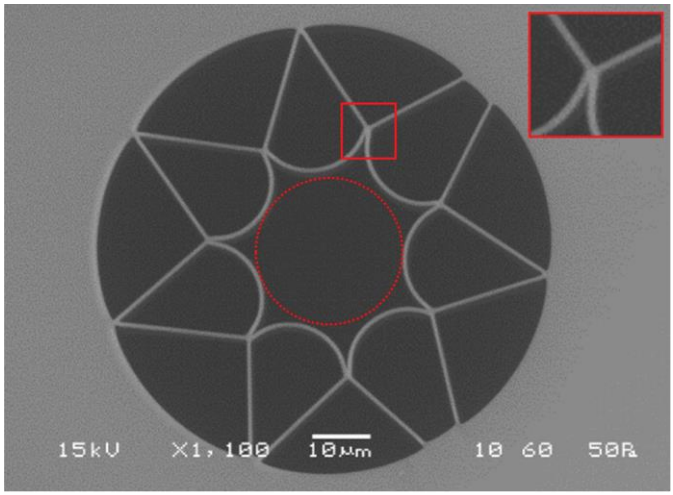

(a)

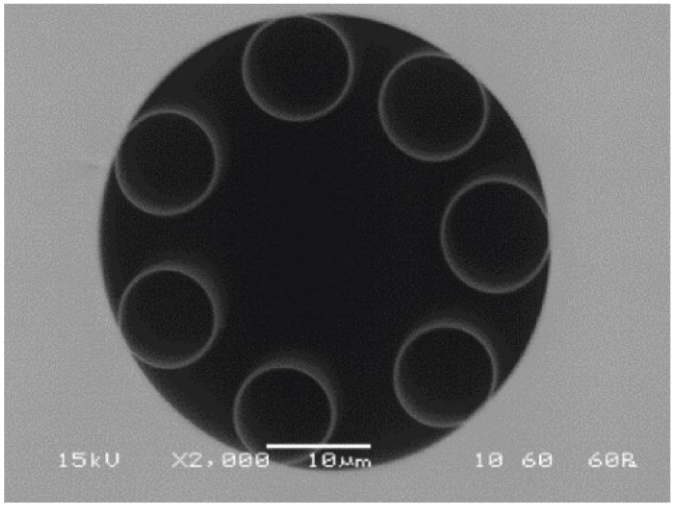

(b)

Fig. 1. Cross-section of the investigated NC-ARFs: (a) NCF fiber with an inscribed circle indicating core diameter, inset – magnified area of the glass node, (b) OBF fiber (SEM).

This article has been accepted for publication in a future issue of this journal, but has not been fully edited. Content may change prior to final publication. Citation information: DOI 10.1109/JLT.2019.2937210, Journal of Lightwave Technology

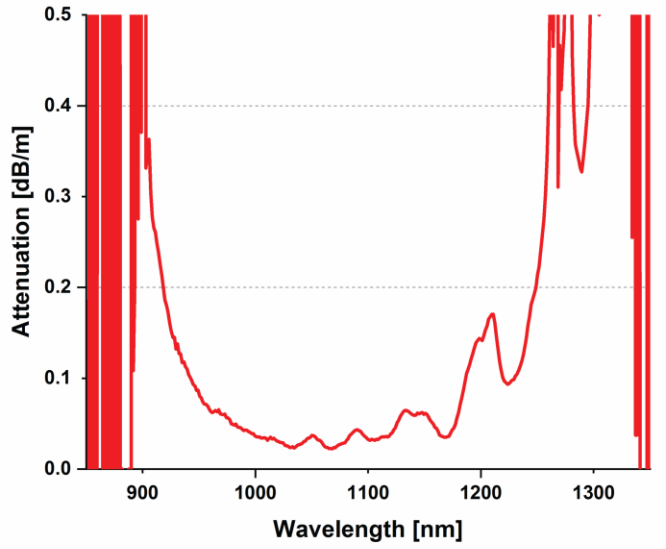

(a)

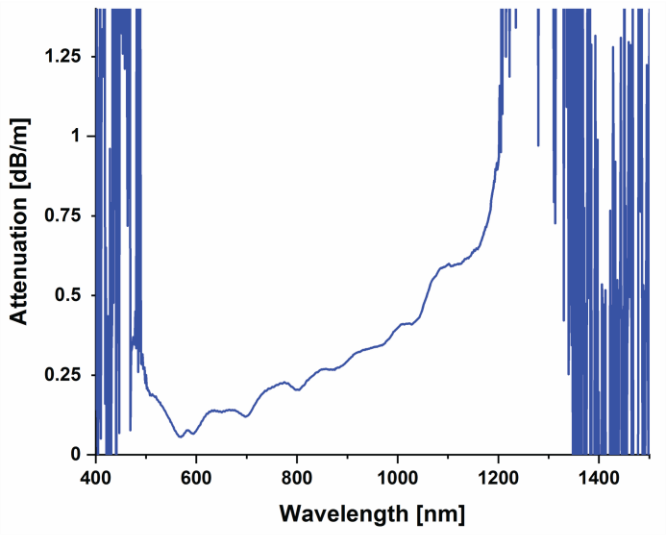

(b)

Fig. 2. Measured attenuation of the (a) NCF fiber, (b) OBF fiber.

This article has been accepted for publication in a future issue of this journal, but has not been fully edited. Content may change prior to final publication. Citation information: DOI 10.1109/JLT.2019.2937210, Journal of Lightwave Technology

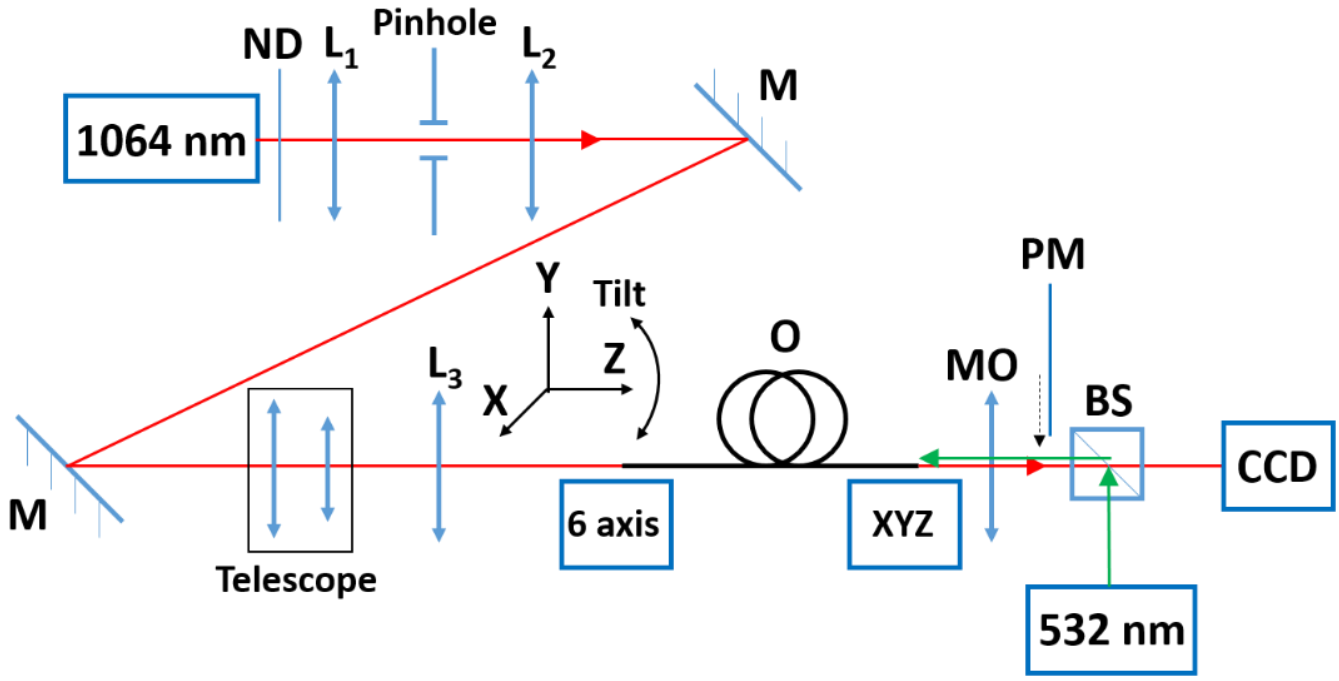

Fig. 3. Transmission measurement setup. Notation: ND – neutral density filter, M – mirrors, L_n – lenses, O – measured fiber, XYZ – 3-axis positioning stage, MO – microscope objective 10x, PM – power meter, BS – beam splitter, CCD – camera.

(a) (b) (c)

Fig. 4. Pictures of the far-field of the output beam, localized inside the (a,b) NCF fiber core under back illumination with the 532 nm laser, (c) OBF fiber core.

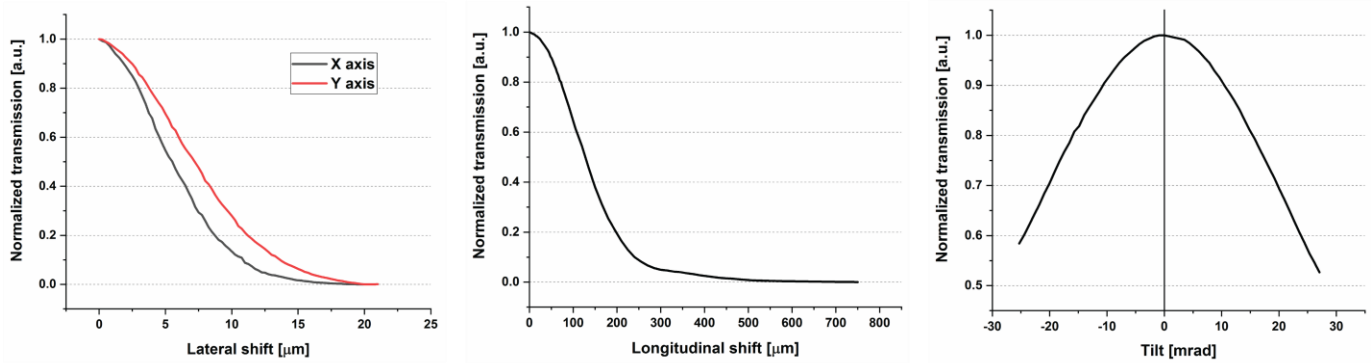

(a) (b) (c)

Fig. 5. Transmission loss of the NCF fiber as a function of input coupling misalignment for (a) X (horizontal) and Y (vertical) axis, (b) Z (longitudinal) axis, and (c) angular.

This article has been accepted for publication in a future issue of this journal, but has not been fully edited. Content may change prior to final publication. Citation information: DOI 10.1109/JLT.2019.2937210, Journal of Lightwave Technology

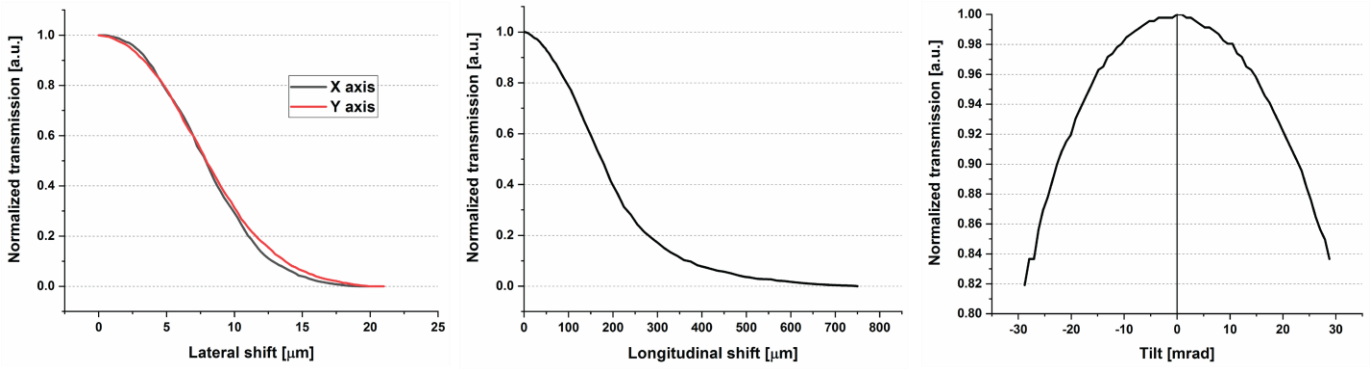

(a) (b) (c)

Fig. 6. Transmission loss of the OBF fiber as a function of input coupling misalignment for (a) X (horizontal) and Y (vertical) axis, (b) Z (longitudinal) axis, and (c) angular.

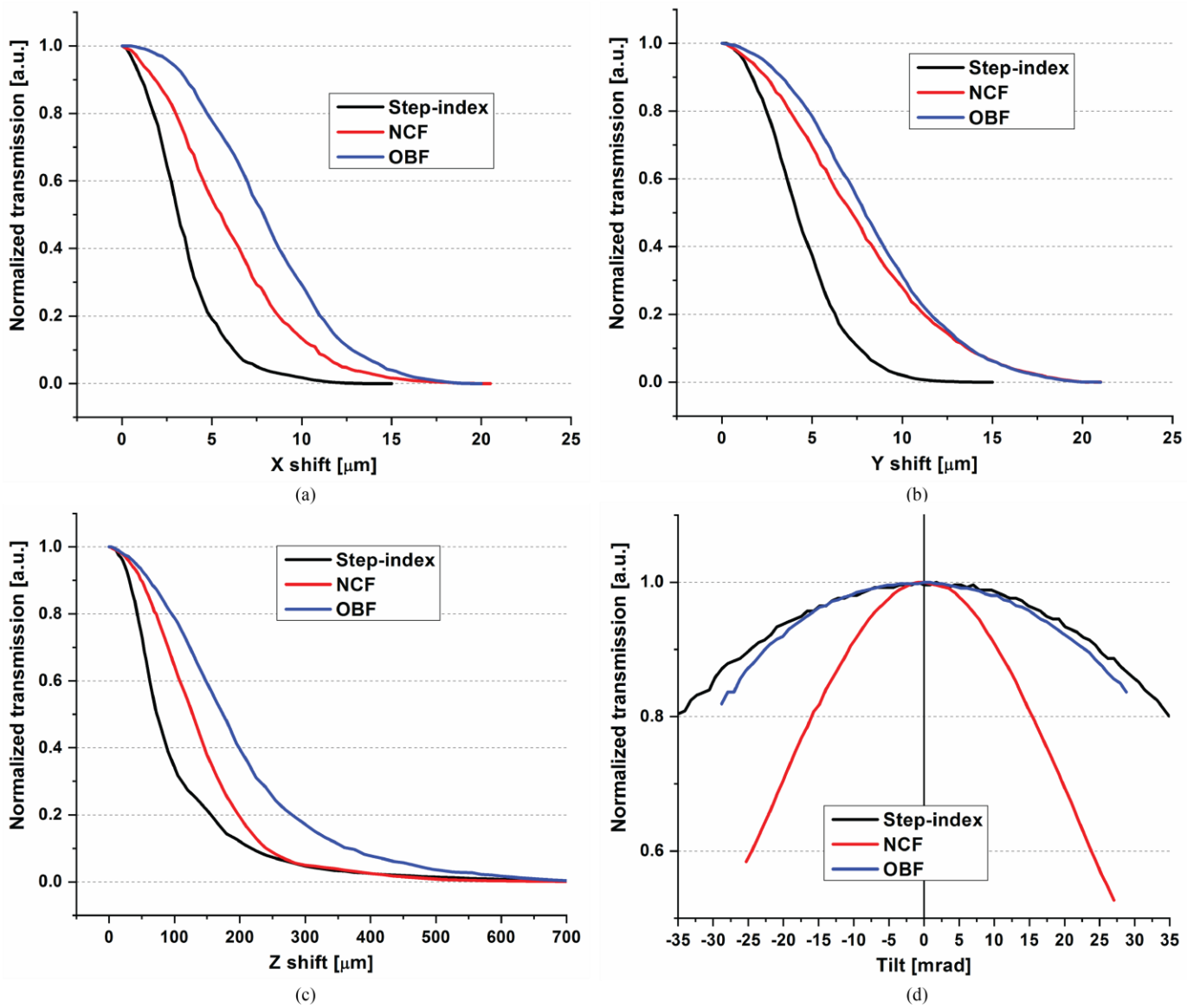

(a) (b) (c) (d)

Fig. 7 Comparison of transmission loss as a function of input coupling misalignment between step-index fiber and NC-ARFs. (a) X (horizontal) axis, (b) Y (vertical) axis, (c) Z (longitudinal) axis, and (d) the pitch.

This article has been accepted for publication in a future issue of this journal, but has not been fully edited. Content may change prior to final publication. Citation information: DOI 10.1109/JLT.2019.2937210, Journal of Lightwave Technology

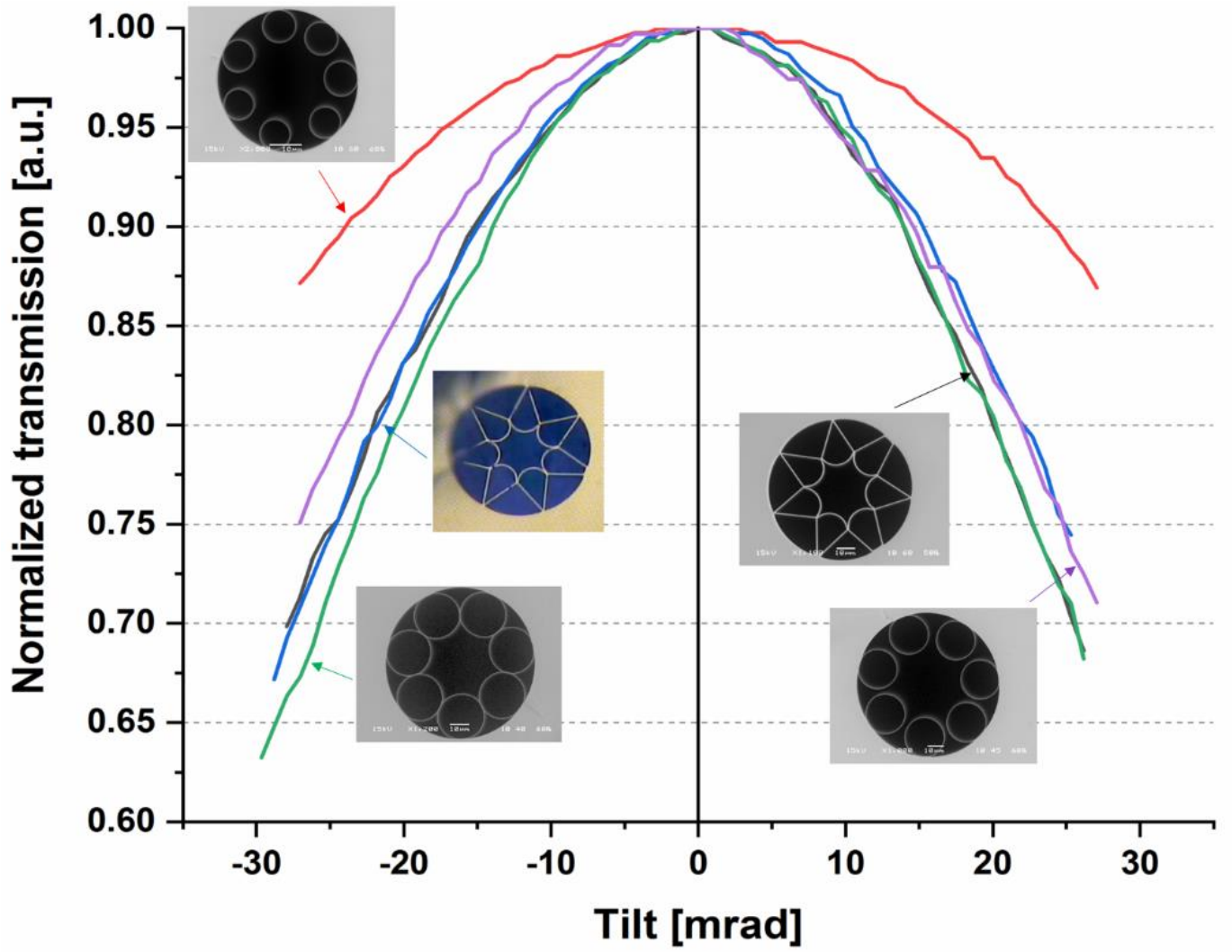

Fig. 8 Comparison of various NCF- and OBF-type of fibers sensitivity to tilt. Red and black curves represent the OBF and NCF fibers respectively, investigated in this work.

TABLE I
SHIFT OF POSITION OF INVESTIGATED FIBERS TIP RESULTING IN 10% DECREASE OF TOTAL OUTPUT POWER OF THE BEAM, FOR FOUR DEGREES OF FREEDOM

Fibre	X [µm]	Y [µm]	Z [µm]	Tilt [mrad]
Step--index	1.74	1.70	31.5	24.5
NCF	1.76	2.50	48.0	10.5
OBF	3.50	3.40	63.0	22.0

This article has been accepted for publication in a future issue of this journal, but has not been fully edited. Content may change prior to final publication. Citation information: DOI 10.1109/JLT.2019.2937210, Journal of Lightwave Technology

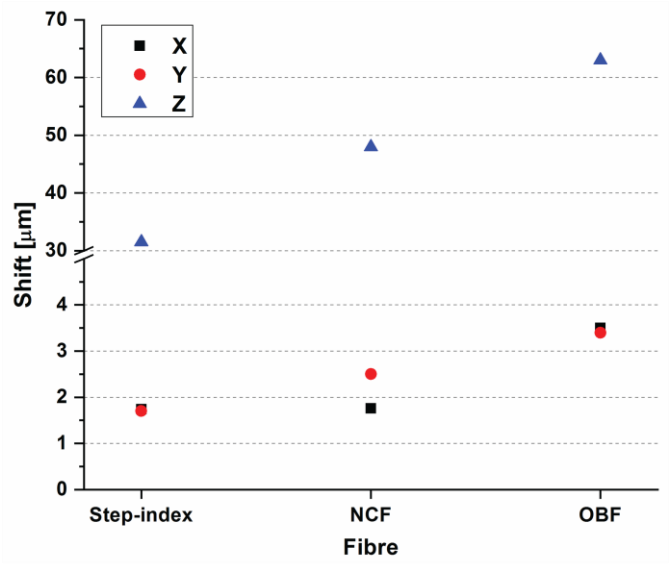

(a)

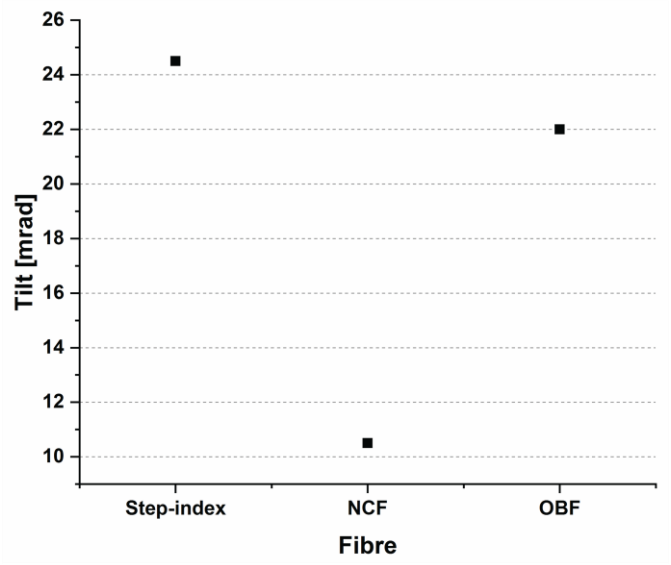

(b)

Fig. 9 Linear and angular shifts of the fiber tip resulting in 10% coupling loss, for four degrees of freedom, data from Table 1. (a) Linear shift, (b) Angular tilt.

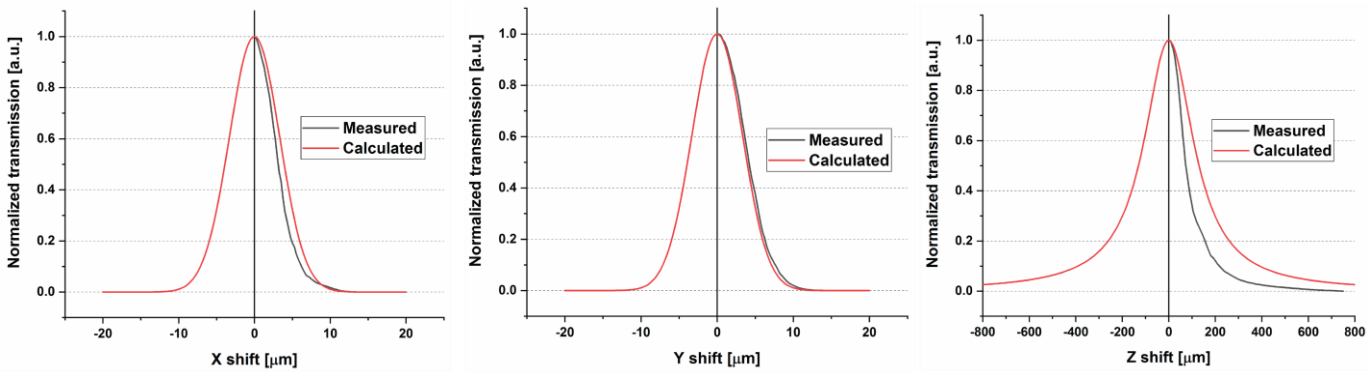

(a) (b) (c)

Fig. 10 Calculated and measured profiles of total transmission normalized to maximum in the step-index fiber as a function of input beam shift in the (a) X (horizontal), (b) Y (vertical), and (c) Z (longitudinal) axis.

This article has been accepted for publication in a future issue of this journal, but has not been fully edited. Content may change prior to final publication. Citation information: DOI 10.1109/JLT.2019.2937210, Journal of Lightwave Technology

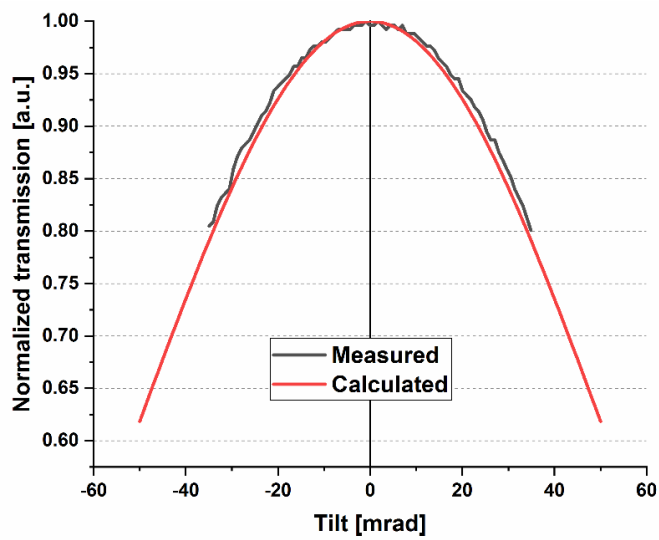

Fig. 11 Calculated and measured profile of total transmission normalized to maximum in the step-index fiber as a function of input beam tilt, while compensating for unwanted shift in Y.